BULLETIN OF THE EARTHQUAKE
RESEARCH INSTITUTE
Vol. 44 (1966), pp. 939-964

49. *World-Wide Survey of the Regional Characteristics of Group Velocity Dispersion of Rayleigh Waves.*

By Tetsuo SANTÔ,
International Institute of
Seismology and Earthquake Engineering, Tokyo
and
Yasuo SATÔ,
Earthquake Research Institute.

(Read June 28, 1966.-Received June 30, 1966.)

Abstract

Group velocity of Rayleigh waves was investigated along more than 200 paths over the vast area including Eurasia, Africa, Atlantic Ocean and Indian Ocean. It was found that Rayleigh wave group velocity could be numerically composed of a number of "standard dispersion curves". Utilizing this fact, the earth's surface was divided into twelve regions each having the standard dispersion character. Together with the previous results for Pacific Ocean area, a map was compiled which shows the regional characteristics of group velocity dispersion of Rayleigh waves. The results were well certificated by least square method. Division pattern thus obtained has, in general, good correlation with topographical conditions. Some exceptional regions, however, were revealed, from which discussions were made.

1. Introduction

In 1961, one of the present writers[1] introduced a technique, which we call "*crossing-path technique*" here. This is a method to divide a wide area into several regions having the same dispersion character of the velocity of surface waves.

1) T. SANTÔ, "Division of the South-western Pacific Area into Several Regions in each of which Rayleigh Waves have the Same Dispersion Characters," *Bull. Earthq. Res. Inst.*, **39** (1961), 603.

The idea of this technique came into mind from the following two evidences.

1) Much of the observed dispersion data of Rayleigh wave group velocity could be classified into a number of "*standard dispersion curves*".

2) Any of the observed dispersion curves can be assumed to have resulted from a mixed path composed of different dispersion regions, in which Rayleigh waves have the standard dispersion curves.

Such relations presented the writer with the possibility to divide a path into several segments having different dispersion characters by the method of "*crossing-path technique*". Details of this procedure is referred to in our previous papers[2),3),4)]. The principle is to divide each travelling path of Rayleigh waves into several different dispersion regions assumed in advance so that the resulted travel-time t_c ($=\sum \Delta_i/V_i$, where V_i represents the group velocity of Rayleigh waves and Δ_i is the length of segment in the region "i") along the path is approximately equal to the observed value t_0. By the trial and error method starting from the basic guidance of topographical map of the area in question, the earth's surface was divided into several regions as shown in Fig. 5. The observed evidences 1) and 2), which are mentioned above, give us a convenience that the division of a certain area into different dispersion regions is sufficient if the procedure is done for the waves with a single period, say 30 seconds.

Establishment of the World-Wide Standardized Seismograph Net (WWSSN) organized by U.S. Coast and Geodetic Survey encouraged one of the writers to extend the technique to wide area other than the Pacific Ocean for which the technique had been successfully applied[5)]. In the present study, the area was extended so as to cover two oceans, Atlantic and Indian, two continents, Eurasia and Africa. The regional characteristics of the group velocity of Rayleigh waves thus discovered in the world-wide area is shown by a newly compiled division map (Fig. 5). A certification of this division map and the discussions on some important results is also given.

---

2) *loc. cit.*, 1).

3) T. SANTÔ, "Division of the Pacific Area into Seven Regions in each of which Rayleigh Waves have the Same Group Velocities," *Bull. Earthq. Res. Inst.*, **41** (1963), 719.

4) T. SANTÔ, "Lateral Variation of Rayleigh Wave Dispersion Character. Part II. Eurasia," *Pure and Applied Geophysics*, **62** (1966), 67.

5) *loc. cit.*, 3).

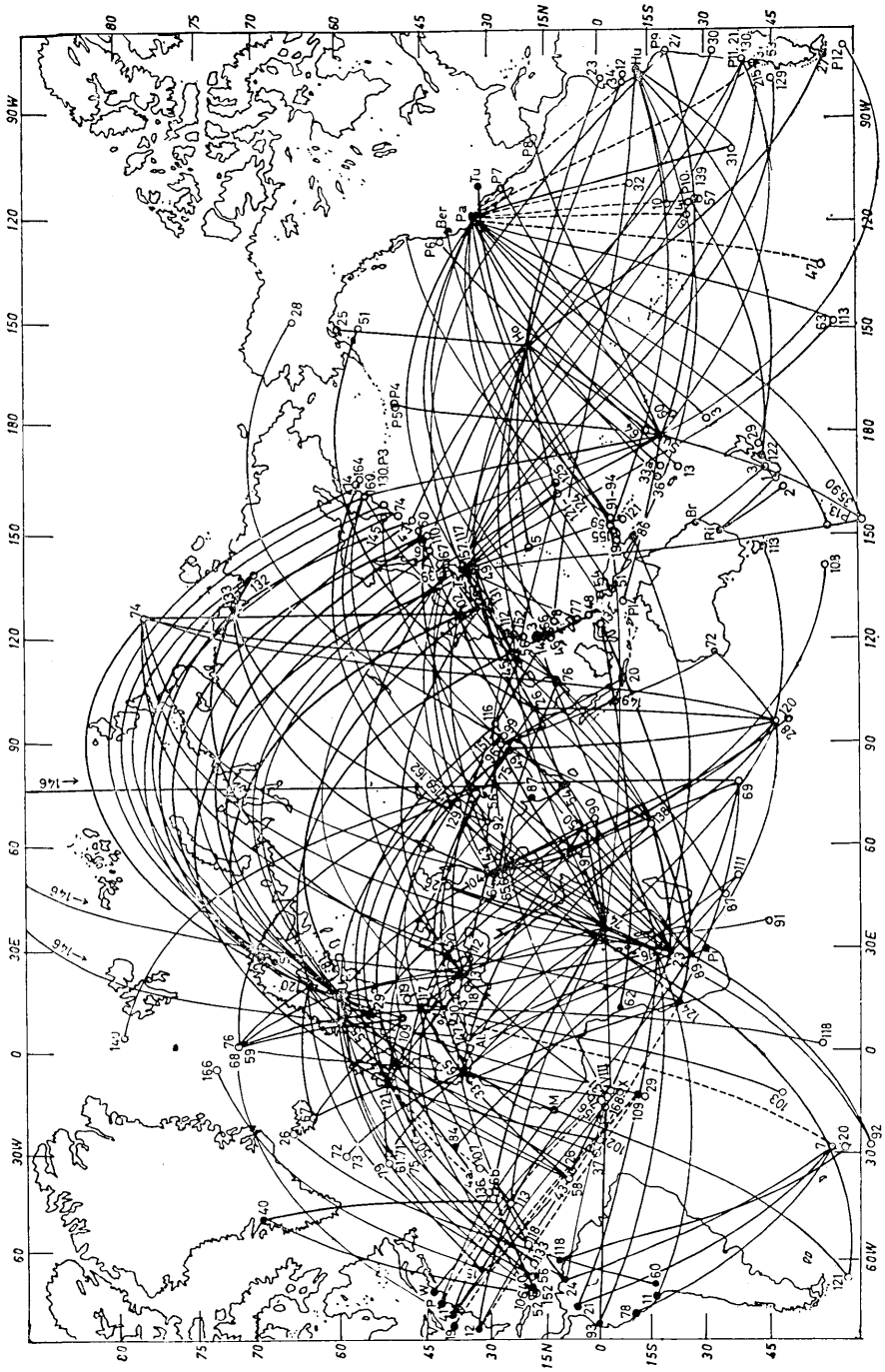

Fig. 1. Travelling paths of Rayleigh waves. Filled circle: Station. Open circle: Epicenter. Dashed curve: The path along which Rayleigh waves showed special type of dispersion.

2. Observational results

Group velocity dispersion data of Rayleigh waves used in the present study originated from

1) Seismograms of WWSSN along 187 paths.
2) Previous data covering sufficient period range by other authors.
3) Previous data by one of the present writers.

(See Fig. 1).

Earthquake data and observation stations are given respectively in Table 1-a), -b) and 3-a). Except for the cases in which paths cross over a certain region (dotted paths in Fig. 1), almost all the dispersion data lie well along the standard dispersion curves. Examples are given in Fig. 2-a). Along the paths crossing mountainous regions, group velocity of Rayleigh waves is lower than that which is given by the curve "*7*", the lowest one for oceanic paths in the Pacific area. In order to represent the dispersion characteristics of these areas, new

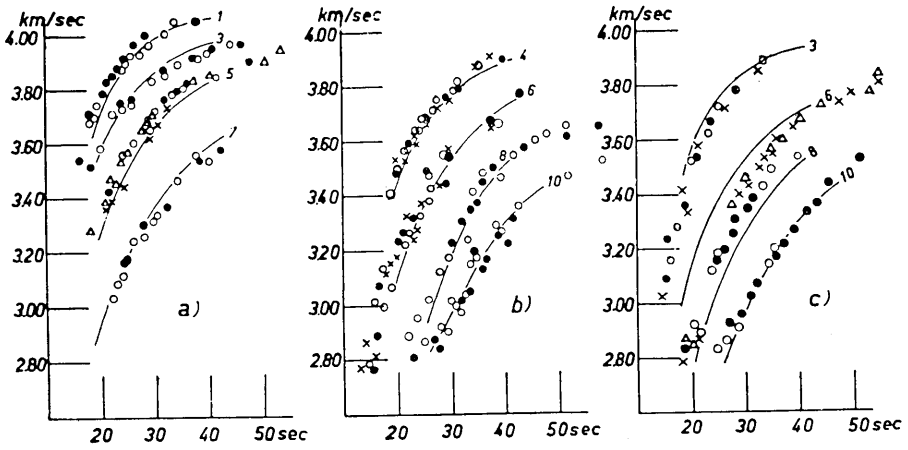

Around 1 :
● 32—89 ○ 31—89
Around 3 :
● 16—19 ○ 17—19
Around 5 :
● 20—74 ○ 21—74
× 7—74 △ 92—74
Around 7 :
● 27—74 ○ 12—74

Around 4 :
● 43—120 ○ 39—120 × 37—120
Around 6 :
● 75—109 ○ 61—109 × 62—109
Around 8 :
● 36—120 ○ 48—120
Around 10 :
● 65—45 ○ 64—45

Around 3 :
● 75—121 ○ 71—121 × 61—121
Below 6 :
× 66—124 △ 65—124
Above 8 :
● 163—92 ○ 164—92
Around 10 :
● 116—29 ○ 99—29

Fig. 2. Some examples of group velocity dispersion data of Rayleigh waves. Several "*Standard dispersion curves*" are presented by solid curves for reference.

Table 1-a). Data of earthquakes used for the area including Eurasia, Africa, Atlantic Ocean and Indian Ocean.

No.	Date	Origin Time GMT	Epicenter *deg.*		Region
		h m s			
2	July 30 '63	13 51 57.8	55.9S	27.5W	Sandwich Islands
12	Aug. 29 '63	08 53 48.4	39.6N	74.2E	Sinkiang Province, China
19	Sept. 23 '63	06 40 36.5	16.6S	38.6E	Northern Rhodesia
18	Sept. 29 '63	22 16 38.6	36.1N	18.0E	Ionian Sea
20	Oct. 03 '63	15 48 17.2	58.5S	25.1W	Sandwich Islands
26	Oct. 15 '63	09 59 30.1	67.2N	18.4W	North of Iceland
28	Mar. 05 '64	06 00 41.3	45.2S	96.4E	Indian Ocean
31	Mar. 14 '64	16 36 52.1	1.9S	12.9W	Mid-Atlantic Ocean
33	Mar. 15 '64	22 30 26.0	36.2S	7.6W	West of Gibraltar
37	July 11 '64	11 52 25.0	1.0N	39.3W	Mid-Atlantic Ocean
40	July 14 '64	09 55 24.4	19.0N	66.5W	Puerto Rico
43	Sept. 04 '64	03 28 33.1	7.6N	36.9W	Central Mid-Atlantic Ridge
48	Oct. 12 '64	15 42 54.7	3.0N	126.7E	Talaud Islands
49	Oct. 14 '64	04 04 59.6	33.4N	141.8E	Off east coast of Honshu, Japan
50	Oct. 18 '64	09 06 26.0	2.9N	65.7E	Carlesberg Ridge
51	Aug. 02 '64	08 36 16.9	56.2N	149.9W	Alaska
52	Aug. 03 '64	01 48 23.3	16.8N	70.7W	Dominican Republic
56	Aug. 10 '64	01 10 12.4	19.1N	67.3W	Mona Passage
58	Aug. 14 '64	21 27 41.6	7.4N	36.8W	Central Mid-Atlantic Ridge
59	Aug. 17 '64	15 15 18.9	72.2N	1.7E	Norwegian Sea
60	Aug. 17 '64	11 51 19.3	46.3N	151.9E	Kurile Islands
61	Aug. 17 '64	22 47 32.4	52.1N	30.1W	North Atlantic Ridge
64	Aug. 19 '64	15 20 13.9	28.2N	52.7E	Southern Iran
65	Aug. 19 '64	09 33 10.0	28.2N	52.6E	Southern Iran
66	Aug. 19 '64	22 40 17.9	28.4N	52.7E	Southern Iran
67	Aug. 20 '64	03 56 29.2	63.9N	20.5W	Iceland
69	Aug. 20 '64	12 48 47.7	37.4S	78.3E	Mid-Indian Ridge
71	Aug. 22 '64	17 04 31.2	51.9N	30.0W	North Atlantic Ridge
73	Aug. 23 '64	04 47 46.6	59.4N	30.2W	North Atlantic Ridge
74	Aug. 25 '64	13 47 20.6	78.2N	126.6E	East of Severnaya Zemlya
75	Aug. 26 '64	03 18 44.1	52.1N	30.1W	North Atlantic Ridge
76	Aug. 20 '64	16 29 58.5	72.3N	1.7E	Norwegian Sea
79	July 24 '64	06 50 52.8	46.9N	153.9E	Kurile Islands
90	Aug. 18 '64	11 09 43.4	0.5N	67.2E	Carlesberg Ridge

(to be continued)

(continued)

No.	Date	Origin Time GMT	Epicenter *deg.*		Region
		h m s			
91	Aug. 18 '64	15 26 11.5	5.7N	58.0E	Carlesberg Ridge
92	Aug. 19 '64	01 30 57.4	61.2S	27.2W	South Sandwich Islands
96	Aug. 30 '64	02 35 08	27.6N	88.3E	Sikkim
99	Sept. 01 '64	13 22 36.6	27,2N	92.3E	India-China border
102	Sept. 05 '64	12 27 22.2	00.6N	25.9W	Central Mid-Atlantic Ridge
103	Sept. 06 '64	03 38 48.8	46.7S	13.5W	South Atlantic Ridge
108	Sept. 05 '64	11 55 37	54.0S	141.1E	West of Macquarie Islands
109	Oct. 01 '64	02 33 03	10.5S	13.3W	Ascension Island
110	Oct. 16 '64	06 59 38.6	44.3N	149.5E	Kurile Islands
111	Oct. 17 '64	08 06 17.2	37.2S	52.2E	South Indian Ocean
112	Oct. 17 '64	09 50 29.5	35.0N	25.4E	Crete
113	Oct. 17 '64	14 48 10.9	26.7N	44.6W	North Atlantic Ridge
116	Oct. 21 '64	23 09 18.8	28.1N	93.1E	India-China border
117	Oct. 22 '64	09 54 36.9	36.7N	141.1E	Near east coast of Honshu, Japan
118	Oct. 23 '64	01 56 03.2	19.8N	56.0E	North Atlantic Ocean
119	Oct. 27 '64	19 46 12.0	47.8N	16.1E	Austria
120	Oct. 27 '64	21 24 31.2	45.6S	96.1E	Southeast Indian Rise
121	Oct. 27 '64	22 36 18	58.5S	66.2W	Drake Passage
126	Nov. 09 '64	08 05 48.8	39.8N	48.8E	Northeastern Iran USSR border
131	Aug. 17 '63	11 12 41.2	30.6N	130.9E	Ryukyu Islands
132	Aug. 19 '62	23 16 07.3	69.8N	138.6E	Siberia
133	July 21 '64	09 56 16.6	72.1N	130.2E	Laptev Sea
134	Nov. 23 '64	22 15 47.0	0.1S	124.5E	Molucca Sea
136	Dec. 02 '64	08 20 45.6	30.6N	42.0E	North Atlantic Ridge
138	Dec. 03 '64	03 50 01.2	15.0S	66.8E	Mid-Indian Rise
139	Dec. 10 '64	15 11 05.8	40.4N	138.9E	Eastern Sea of Japan
140	Dec. 01 '64	07 39 50.2	79.5N	3.9E	Greenland Sea
143	Dec. 22 '64	04 36 34.7	28.2N	57.9E	Southern Iran
145	Dec. 26 '64	14 30 29.1	51.8N	156.8E	Kamchatka
146	Dec. 28 '64	17 04 57.0	86.7N	68.7E	North of Franz Josef Land
147	Jan. 01 '65	21 38 29.2	35.7N	4.4E	Algeria
149	Jan. 12 '65	20 50 12.3	5.5S	102.5E	Southern Sumatra
150	Jan. 12 '65	20 31 01.8	46.7N	27.5W	North Atlantic Ridge
151	July 12 '65	13 32 24.0	27.6N	88.0E	Nepal
152	Jan. 15 '65	18 34 07.6	23.6N	121.7E	Taiwan
155	Dec. 24 '64	18 45 45.5	4.4S	153.1E	New Ireland

(to be continued)

(continued)

No.	Date	Origin Time GMT	Epicenter *deg.*		Region
		h m s			
156	Jan. 15 '65	19 24 33	2.0S	12.8W	North of Ascension Island
157	Jan. 23 '65	21 51 14.9	36.9N	140.9E	Near east coast of Honshu, Japan
159	Jan. 26 '65	20 06 02.4	35.6N	73.6E	Northwestern Kashmir
160	Jan. 29 '65	09 35 25.7	54.8N	161.7E	Near east coast of Kamchatka
162	Feb. 02 '65	15 56 51.0	37.5N	73.4E	Tadzhik SSR
164	Feb. 08 '65	15 46 49.9	55.1N	165.7E	Komandorsky Islands
166	Feb. 14 '65	19 37 17.8	73.0N	6.5E	Greenland Sea
167	Feb. 16 '65	12 24 08.8	39.5N	141.8E	Honshu, Japan
168	Feb. 11 '65	04 42 00.7	1.3S	14.4W	North of Ascension Island

Table 1-b). Data of earthquakes previously used.

No.	Date	Origin Time GMT	Epicenter *deg.*		Author
		h m s			
Kam.	May 04 '59	67 15 42	52.5N	159.5E	M. T. Porrka[6]
14	June 02 '61	01 13 25.4	50.1N	164.8E	T. Santô[7]
130	Oct. 13 '60	14 52 34.7	54.8N	161.2E	〃
127	Oct. 28 '60	13 18 14.3	52.0N	157.4E	〃
74	Jan. 16 '61	14 22 18.2	49.9N	156.2E	〃
10	June 15 '61	23 24 40.4	45.4N	151.3E	〃
72	Feb. 12 '61	21 53 43.5	43.7N	147.7E	〃
43	Aug. 11 '61	15 51 35.4	42.9N	145.1E	〃
145	Mar. 23 '60	00 23 22	39.5N	143 E	〃
73	Jan. 16 '61	15 41 23.3	39.4N	140.6E	〃
6b	Oct. 23 '50	16 40 36	32 N	41 W	J. E. Oliver et al.[8]
4a	July 25 '50	18 15 00	31 N	42 W	〃
III	Aug. 23 '53	07 18 06	1 S	14 W	H. Berckhemer[9]
VII	July 9 '53	21 23 48	30 N	42.5W	〃

(to be continued)

6) M. T. Porkka, "Surface Wave Dispersion for Some Eurasian Paths. I. Rayleigh Waves from Kamchatka and Japan to Finland," *Geophysica*, **7** (1960), 101.

7) T. Santô, "Dispersion of Surface Waves along Various Paths to Uppsala, Sweden. Part I. Continental Paths," *Ann. di Geofis.*, **15** (1962), 243.

8) J. E. Oliver, M. Ewing and F. Press, "Crustal Structure and Surface-Wave Dispersion, Part IV. Atlantic and Pacific Ocean Basins," *Bull. Geol. Soc. Amer.*, **66** (1955), 913.

9) H. Berckhemer, "Rayleigh-Wave Dispersion and Crustal Structure in the East Atlantic Ocean Basins," *Bull. Seism. Soc. Amer.*, **46** (1956), 83.

(continued)

No.	Date	Origin Time GMT	Epicenter *deg.*		Author
		h m s			
26	Aug. 30 '61	03 35 07.7	7.0N	33.2W	T. Santô[10]
79	Apr. 30 '61	07 33 53.5	52.0N	31.9W	〃
133	May 31 '60	11 02 20	18 N	62 W	〃
152	June 08 '62	01 00 24.2	18.5N	70.5W	〃
VIII2	Mar. 26 '62	12 04 54.6	0.5S	19.2W	H. A. Ossing[11]
VIII3	Apr. 15 '62	18 08 27.3	2.7S	11.6W	〃
IX2	Sept. 12 '62	23 58 46.8	7.3S	13.3W	〃
Alg.	Sept. 9 '54	01 04 37	36.3N	1.5E	F. Press et al.[12]
〃	Sept. 10 '54	05 44 05	36.6N	1.3E	〃
91	Dec. 26 '61	06 17 30.6	44.2S	38.1E	T. Santô[13]
118	July 13 '60	07 55 54	53.5S	1.5E	〃
29	Aug. 16 '61	16 15 57.5	13.8S	14.7W	〃
87	July 26 '58	06 13 50	40 S	45.5E	T. Santô[14]
7b	Oct. 31 '50	19 15 22	1 N	26 W	J. E. Oliver et al.[15]
107	June 08 '60	16 19 48	35 N	35 W	T. Santô[16]

Table 2. Data of earthquakes used for Pacific Area.
(Numbers and/or notations of earthquakes were all taken from the original papers.)

No.	Date	Origin Time GMT	Epicenter *deg.*		Author
		h m s			
1	Aug. 08 '47	05 32 48	46 S	166 E	C. B. Officer[17]
2	Feb. 06 '50	22 53 00	48 S	164 E	〃
3	June 19 '48	07 05 36	43.2S	169.3E	〃
4	Sept. 22 '50	07 52 07	25 S	114 W	〃

(to be continued)

10) T. SANTÔ, "Dispersion of Surface Waves along Various Paths to Uppsala Sweden. Part II. Arctic and Atlantic Oceans," *Ann. di Geofis.*, **15** (1962), 277.

11) H. A. OSSING, "Dispersion of Rayleigh Waves Originating in the Mid-Atlantic Ridge," *Bull. Seism. Soc. Amer.*, **54** (1964), 1137.

12) F. PRESS, M. EWING and J. OLIVER, "Crustal Structure and Surface Wave Dispersion in Africa," *Bull. Seism. Soc. Amer.*, **46** (1956), 97.

13) *loc. cit.*, 10).

14) T. SANTÔ, "Observation of Surface Waves by Columbia-type Seismograph Installed at Tsukuba Station, Japan. Part 1. Rayleigh Waves Dispersion Across the Ocean Basin," *Bull. Earthq. Res. Inst.*, **38** (1960), 219.

15) *loc. cit.*, 8).

16) *loc. cit.*, 10).

17) C. B. OFFICER, "Southwest Pacific Crustal Structure," *Trans. Amer. Geophys. Union*, **36** (1955), 449.

(continued)

No.	Date	Origin Time GMT	Epicenter *deg.*	Author
		h m s		
5	June 13 '47	20 24 51	19 N 146 E	J. E. Oliver[18]
28	Dec. 29 '49	03 03 55	18.5N 121½E	M. Ewing et al.[19]
42A	Oct. 22 '51	03 29 26	24 N 122½E	〃
35	Nov. 5 '50	17 37 27	33.3N 134.8E	〃
43	Nov. 6 '51	16 40 06	47 N 154 E	〃
16	Sept. 10 '48	13 48 34	43.5N 147 E	〃
25	Sept. 27 '49	15 30 43	60 N 149 W	〃
64	Dec. 26 '49	06 23 54	14.5S 180 E	〃
33a	Oct. 4 '50	00 41 07	18.5S 170 E	〃
17	Mar. 16 '49	22 15 13	5.5S 151 E	〃
23	Aug. 5 '49	19 08 47	1 S 78 W	〃
2	Nov. 10 '46	17 43 00	7.8S 77.8W	〃
27	Dec. 17 '49	15 07 53	54 S 71 W	〃
21	Apr. 20 '49	03 29 00	38 S 72.5W	〃
56	Dec. 16 '41	19 19 39	21.5N 120.5E	T. Santô et al.[20]
46	Apr. 8 '42	15 40 24	13.5N 121.5E	〃
08	May 3 '43	01 59 12	12.5N 125.5E	〃
54	Sept. 12 '41	07 02 04	0.5S 132.5E	〃
51	Jan. 27 '42	13 29 08	4.5S 135 E	〃
19	May 12 '38	15 38 57	6 S 147.8E	〃
36	Jan. 20 '46	16 54 21	17.5S 167.5E	〃
13	Mar. 14 '43	17 11 00	22 S 169.5E	〃
60	Oct. 24 '43	16 04 36	22 S 174 W	〃
03	Sept. 14 '43	07 18 08	30 S 177 W	〃
35	Mar. 23 '45	23 14 13	62 S 153 E	〃
63	Sept. 5 '38	14 42 32	55 S 152 W	〃
47	Feb. 14 '41	18 55 16	53.5S 131 W	〃
57	Jan. 2 '40	11 07 14	28.5S 113 W	〃
31	Sept. 22 '42	00 46 15	37 S 98 W	〃
32	July 23 '39	15 07 24	9 S 109 W	〃
46	Apr. 8 '42	15 40 24	13.5N 121 E	〃
59	Jan. 13 '41	16 27 38	4.5S 152.5E	〃
51	Jan. 27 '42	13 29 08	4.5S 135 E	〃
29	Aug. 1 '42	12 34 03	41 S 175.8E	〃
31	Sept. 22 '42	00 46 15	37 S 98 W	〃
6	Feb. 19 '51	22 11 54	25 S 117 W	R. L. Kovach et al.[21]
10	Dec. 15 '51	01 19 02	21.5S 113 W	〃

(to be continued)

18) *loc. cit.*, 8).

19) M. Ewing and F. Press, "Crustal Structure and Surface Wave Dispersion. Part II. Solomon Islands Earthquake of June 29, 1950," *Bull. Seism. Soc. Amer.*, **42** (1952), 315.

20) T. Santô and M. Båth, "Crustal Structure of Pacific Ocean from Dispersion of Rayleigh Waves," *Bull. Seism. Soc. Amer.*, **53** (1963), 151.

21) R. L. Kovach and F. Press, "Rayleigh Wave Dispersion and Crustal Structure in the Eastern Pacific and Indian Oceans," *Geophys. J.*, **4** (1961), 202.

(continued)

No.	Date	Origin Time GMT	Epicenter *deg.*	Author
		h m s		
124	Jan. 15 '60	09 30 24	15 S 75 W	T. Santô[22]
27	July 11 '58	19 10 20	21 S 69 W	〃
30	Sept. 4 '58	21 51 08	33.5S 69.5W	〃
139	Apr. 15 '60	03 25 38	27 S 113 W	〃
215	June 8 '60	08 12 24	42.4S 74.8W	〃
130	May 28 '60	11 05 40	38 S 73 W	〃
129	May 28 '60	23 06 55	45 S 77 W	〃
113	Nov. 29 '59	19 17 40	57 S 147.5W	〃
90	Dec. 01 '59	14 59 40	63 S 154 E	〃
121	Feb. 24 '60	21 37 05	7.5S 156 E	〃
19	May 25 '58	21 11 45	12 N 165 E	〃
77	Sept. 11 '58	18 01 45	7 N 126.5E	〃
91	July 29 '50	23 40 08	6.8S 155.1E	M. Ewing et al.[23]
92	July 29 '50	23 49 08	6.8S 155.1E	〃
93	July 29 '50	23 49 08	6.8S 155.1E	〃
94	July 29 '50	23 49 08	6.8S 155.1E	〃
P1	Mar. 23 '60	00 23 22	39.5N 143 E	J. Kuo et al.[24]
P2	Oct. 27 '59	06 52 50	45.5N 151 E	〃
P3	Dec. 27 '59	15 52 55	56 N 162.5E	〃
P4	May 20 '58	01 38 04	51 N 173 W	〃
P5	Feb. 22 '58	10 50 23	50.5N 175.5W	〃
P6	Aug. 6 '60	07 39 22.6	40 N 126.6W	〃
P7	Apr. 12 '58	11 46 58	26.5N 111 W	〃
P8	May 22 '59	19 12 40	17.5N 97 W	〃
P9	Apr. 15 '58	19 14 29	16.5S 71.5W	〃
P10	Apr. 15 '60	03 25 36	27 S 113 W	〃
P11	June 20 '60	02 01 08	38 S 73.5W	〃
P12	Feb. 8 '60	12 45 34	58 S 67 W	〃
P13	Mar. 22 '60	02 31 17	61.5S 154 E	〃
P14	Oct. 7 '60	15 18 80.8	7.4S 130.7E	〃
121	June 28 '58	19 30 00.1	11.4N 162.1E	P. W. Pomeroy[25]
122	June 28 '58	19 30 00.1	11.4N 162.1E	〃
123	June 28 '58	19 30 00.1	11.4N 162.1E	〃
124	June 28 '58	19 30 00.1	11.4N 162.1E	〃
125	July 12 '58	03 30 00.1	11.4N 165.2E	〃

22) *loc. cit.*, 3).

23) *loc. cit.*, 19).

24) J. KUO, J. BRUNE and M. MAJOR, "Rayleigh Wave Dispersion in the Pacific Ocean for the Period Range 20 to 140 Seconds," *Bull. Seism. Soc. Amer.*, **52** (1962), 333.

25) P. W. POMEROY, "Long Period Seismic Waves from Large, Near-Surface Nuclear Explosions," *Bull. Seism. Soc. Amer.*, **53** (1963), 109.

Table 3-a). List of stations for the earthquakes in Table 1-a) and -b).

No. Abbr.	Station	Region	Latitude	Longitude
10	L' Aquila	Italy	42°21′14″N	13°25′11″E
11	Arequipa	Peru	16 27 44 S	72 29 29 W
12	Atlanta	Georgia	33 26 N	84 20 15 W
13	Athens	Greece	37 58 22 N	23 43 E
14	Bagio City	Philippines	16 24 39 N	120 34 47 E
15	Bermuda	Bermuda	32 22 46 N	64 40 52 W
19	Blacksburg	Virginia	37 12 40 N	80 25 14 W
20	Lembang	Java	06 50 S	107 37 E
21	Botota	Colombia	4 37 23 N	74 03 54 W
23	Bulawayo	Rhodesia	20 08 36 S	28 36 48 E
24	Caracas	Venezuela	10 30 24 N	66 55 40 W
26	Chiengmai	Thailand	18 47 24 N	98 58 37 E
28	College	Alaska	64 54 N	147 48 36 W
29	Copenhagen	Denmark	55 41 N	12 26 E
40	Godhavn	Greenland	69 15 N	53 32 W
41	Georgetown	Washingtion, D. C.	38 54 N	77 04 W
45	Hong Kong	Hong Kong	22 18 13 N	114 10 19 E
50	Istanbul	Turkey	41 02 36 N	28 59 06 E
52	Kevo	Finland	69 45 21 N	27 00 45 E
54	Kodaikanal	India	10 14 N	77 28 E
55	Kongsberg	Norway	59 38 57 N	09 37 55 E
60	La Paz	Bolivia	16 31 58 S	68 05 54 W
62	Luanda	Angola	08 59 S	13 14 E
65	Malaga	Spain	36 43 39 N	04 24 40 W
66	Manila	Philippines	14 40 N	121 05 E
72	Mundaring	Australia	31 58 30 S	116 12 24 E
74	Nairobi	Kenya	01 16 26 S	36 48 13 E
75	New Delhi	India	28 41 N	77 13 E
76	Nhatrang	South Viet-Nam	12 12 36 N	109 12 42 E
78	Nana	Peru	11 59 15 S	76 50 32 W
81	Nurmijarvi	Finland	60 30 32 N	24 39 05 E
84	Ponta Delgada	Azores	37 44 36 N	25 39 42 W
86	Port Moresby	New Guinea	09 24 33 S	147 09 14 E
89	Pretoria	South Africa	25 45 S	28 15 E
92	Quetta	Pakistan	30 11 18 N	66 57 E

(to be continued)

(continued)

No. Abbr.	Station	Region	Latitude	Longitude
93	Quito	Ecuador	00°12′01″S	28°30′02″W
102	Seoul	Korea	37 34 N	126 58 E
104	Shiraz	Iran	29 30 40 N	52 31 34 E
105	Shillong	India	25 34 N	91 53 E
106	San Juan	Puerto Rico	18 06 42 N	66 09 W
109	Stuttgart	Germany	48 46 15 N	09 16 36 E
112	Anpu	Taiwan	25 11 N	121 31 E
113	Tasmania	Tasmania	42 54 36 S	147 19 14 E
117	Triest	Italy	45 42 32 N	13 45 51 E
118	Trinidad	West Indies	10 39 N	61 24 06 W
120	Umeå	Sweden	63 48 54 N	20 14 12 E
121	Valentia	Ireland	10 56 N	10 15 W
124	Windhoek	South Africa	22 32 N	17 09 E
Sod.	Sodankylä	Finland	67 22 16 N	26 37 45 E
Pal.	Palisades	New York	41 00 25 N	73 54 31 W
M'	M' Bour	Senegal	14 23 30 N	16 57 30 W
W	Weston	Massachusetts	42 23 05 N	71 19 20 W
Ts	Tsukuba	Japan	36 12 39 N	140 06 36 E

Table 3-b). List of stations for the earthquakes in Table 2.

No. Abbr.	Station	Region	Latitude	Longitude
Ri	Riverviews	Australia	33°49′46″S	151°09′30″E
Br	Brisbane	Australia	27 23 30 S	152 46 30 E
122	Christchurch	New Zealand	43 31 54 S	172 37 18 E
Ho	Honolulu	Hawaii	21 21 30 N	157 48 35 W
Pa	Pasadena	California	34 08 54 N	118 10 18 W
Hu	Huancayo	Peru	12 02 18 S	75 19 22 W
Ts	Tsukuba	Japan	36 12 39 N	140 06 36 E
Ber	Berkeley	California	37 52 24 N	122 15 36 W
Tu	Tucson	Arizona	32 18 35 N	110 40 56 W
Pal	Palisides	New York	41 00 25 N	73 54 31 W
Su	Suva	Fiji Islands	18 08 56 S	178 27 26 E
45	Hong Kong	Hong Kong	22 18 13 N	114 10 19 E

Table 4. Examples of the divided segments Δi and the comparison of V_C with V_O. Paths are represented by the index numbers of epicenter and station (underlined).

$ti=\Delta i/Vi$, where Vi is group velocity of Rayleigh waves with characteristic number i. $\Delta=\Sigma\Delta i$. $C=\Sigma ti$. O: Observed travel-times of Rayleigh waves along the total path. $V_C=\Delta/\Sigma ti$. V_O: Observed group velocity of Rayleigh waves. (Period: 30 seconds.)

Path	Path-length (km)										Travel-time (sec)										Group velocity (km/sec)		V_C–V_O (km /sec)
	Total	Segment									Segment									Total			
	Δ	Δ_0	Δ_1	Δ_3	Δ_5	Δ_6	Δ_7	Δ_8	Δ_9	Δ_{12}	t_0	t_1	t_3	t_5	t_6	t_7	t_8	t_9	t_{12}	C	O	V_C	V_O	
91– 23	4320	500	900	720	500	1700					123	225	187	137	483					1155	1150	3.74	3.74	−0.01
91– 74	2460				1360	500	600						372	142	179					673	695	3.55	3.55	0.00
91– 75	3200		650	850	800		700		200			163	220	218		208		65		874	872	3.66	3.67	−0.01
91–104	2700				1300	1100			300					355	312			98		765	765	3.53	3.53	0.00
108– 50	14920	3700	3200	1920	2500	2100	1000	100	400		908	802	497	685	597	298	31	131		3949	3922	3.78	3.80	−0.02
111– 23	2950		500	1500	100	850						125	389	27	242					783	783	3.76	3.76	0.00
111– 65	10100		600	1600	300	2400	5000	200				150	414	82	682	1487	61			2876	2850	3.52	3.55	−0.03
116– 89	9200		900	3200	1600	900	2000		200	400		226	830	437	256	597		65	148	2559	2560	3.60	3.60	0.00
116–124	9950		1600	2350	1400	1800	2000		300	500		400	608	383	511	597		98	186	2773	2777	3.44	4.44	0.00
120– 26	7200	4700	300	200			2000				1150	75	52			597				1874	1865	3.84	3.86	−0.02
120– 29	13600				7800	1500	2800	800	700					2131	427	834	247	229		3868	3880	3.52	3.50	+0.02
120– 65	13500		700	2100	4500	3200	2600	400				175	544	1229	910	774	123			3755	3755	3.60	3.60	0.00
120– 75	8400	1200	4700	400	500		1300		300		284	1176	103	137		387	98			2195	2190	3.83	3.84	−0.01
120–121	14800			1400	6000	4300		800	400	1900			363	1640	1220	238	123	622		4206	4210	3.52	3.52	0.00
120– 89	6200	600	1600	3000	500	500					146	400	778	137	142					1602	1600	3.87	3.87	0.00
69–104	7800			800	5700	1000			300				207	1556	284			98		2145	2150	3.64	3.63	+0.01
69– 75	7250	1700	1750	200	1400		2000		200		417	439	52	383		597		65		1953	1940	3.72	3.74	−0.02

standard curves "*8*", "*9*", and "*10*" were added, which have a similar nature to the previously defined dispersion curves. Examples of data with such a low group velocity having been obtained in mountainous regions are given in Figs. 2-b) and 2-c).

Dividing of every path into different segments "i" was made by the trial and error method until the calculated group velocity

$$V_c\left(=\Sigma\Delta_i/\Sigma\left(\frac{\Delta_i}{V_i}\right)\right)$$

approached the observed group velocity V_0 within the limit of observational error, say ± 0.02 km/sec. Examples of the divided segments are given in Table 4, in which comparisons of V_c with V_0 are made in the last column.

Fig. 5 gives the final division pattern showing 14 different dispersion regions together with the previous results for Pacific Ocean area. Exceptional dispersion data which do not follow the standard dispersion curves were observed along the Mid-Atlantic Ridge, for which two special dispersion curves "B'" and "C" (dotted curves in the annexed dispersion diagram of Fig. 5) were assumed. Frequency distribution of V_c-V_0 resulted from the above division is represented in Table 5 for 30 second period. Nearly 90% of V_c-V_0 is successfully distributed in the desired range of ± 0.02 km/sec.

Table 5. Frequency distribution of V_c-V_0 (period: 30 seconds)

V_c-V_0 (km/sec)	Frequency	Percentage
0.05	0	
0.04	3	5.9
0.03	10	
0.02	25	
0.01	23	
0.00	91	89.8
−0.01	41	
−0.02	18	
−0.03	9	
−0.04	1	4.3
−0.05	0	
Σ	221	100

3. Further calculation of the velocity by means of least square method

Our division map was obtained as the result of dividing each path into a number of segments with suitable length Δ_i so that the equations

$$\sum_i \left(\frac{\Delta_i}{V_i}\right) = t_{30} \quad (i=0,1,3,5,\cdots B' \text{ and } C)$$

may be satisfied within observational error, where t_{30} represents the observational travel-time of Rayleigh waves with the period of thirty seconds. In this case, V_i was taken as group velocity for the corresponding period from each standard dispersion curve "i".

Here, however, we assume that V_i in equations (1) are unknowns. Consequently, we have as many simultaneous equations as the number of paths for each period of Rayleigh waves with regard to the group velocity V_i in every dispersion region. Therefore from these equations we can calculate the value of V_i by least square method as functions of period. If our division map is a satisfactory one, the V_i thus obtained must agree well with the group velocities of the corresponding standard curve "i".

The calculations were carried out at the Computer Centre of the University of Tokyo. Table 6 gives a part of numerical data and the results of calculations are given in Table 7 and in Fig. 3.

Except for such a short period as 20 seconds, in which relatively large errors are apt to occur in the measurement of group velocity, concordance of calculated group velocity V_i with that of the "*standard dispersion curves*" is in both cases quite excellent. The coincidence of V_A and V_B for the East Pacific Rise and V_B' and V_C for the Mid-Atlantic Ridge with reference curve "A", "B", "B'" and "C" respectively, however, are not good and have large probable errors.

The following can be supposed as the causes. First the dispersion curves "A", "B", "B'" and "C" were, unlike any other standard dispersion curves, not directly observed. For this reason, there was originally a rather large ambiguity both in the shape of these special regions in the division map as well as in the assumed dispersion curves for these regions.

Second, the numbers of paths crossing the special regions in question were much less than those crossing any other ordinary regions. This makes the weight of coefficient Δ_i of equation (1) for the four unknowns V_A, V_B, $V_{B'}$ and V_C corresponding to the special regions much weaker than

Table 6. Some examples of the numerical data used for calculating the group velocity V_C in every dispersion region. Paths are represented by the index numbers of epicenter and station (underlined).

Observational equations:

$$\frac{\Delta_0}{V_0}+\frac{\Delta_1}{V_1}+\frac{\Delta_3}{V_3}+\frac{\Delta_5}{V_5}+\frac{\Delta_6}{V_6}+\frac{\Delta_7}{V_7}+\frac{\Delta_8}{V_8}+\frac{\Delta_9}{V_9}+\frac{\Delta_{10}}{V_{10}}+\frac{\Delta_{12}}{V_{12}}+\frac{\Delta_{B'}}{V_{B'}}+\frac{\Delta_C}{V_C}=O_T$$

Path	Δi: Lengths of the segments in various dispersion region. (km)												O_T: Observed travel-times. (sec)				
	Δ_0	Δ_1	Δ_3	Δ_5	Δ_6	Δ_7	Δ_8	Δ_9	Δ_{10}	Δ_{12}	$\Delta_{B'}$	Δ_C	O_{20}	O_{25}	O_{30}	O_{35}	O_{40}
113– 24	0	1350	290	1160	0	0	0	0	0	0	0	250	846	792	771	755	743
– 41	800	500	1100	400	0	250	0	0	0	0	0	200	902	864	841	825	—
– 74	1800	700	100	200	2600	2900	300	300	0	0	0	300	2877	2706	2580	2500	2433
– 89	3000	3000	900	0	2600	0	0	0	0	0	0	300	2722	2600	2540	—	—
–117	1700	1000	200	200	0	1300	0	500	0	0	0	600	1627	1528	1470	1437	—
116– 13	0	0	0	0	0	1770	700	1600	0	2300	0	0	2410	2275	2130	2021	1930
– 45	0	0	0	0	0	980	400	350	0	400	0	0	785	722	680	645	—
– 66	0	0	200	400	0	1850	150	300	0	200	0	0	1069	994	937	898	—
– 89	0	900	3200	1600	900	2000	0	200	0	400	0	0	2920	2685	2560	—	—
–121	0	0	0	0	0	3600	1200	1100	400	2000	0	0	—	—	2678	2557	2461
117–104	0	0	0	0	0	3700	500	2200	0	1700	0	0	—	2743	2560	2433	2392
118– 13	1400	1570	900	500	0	2800	0	0	0	0	0	600	2340	2190	2112	—	—
– 29	0	1800	3500	0	0	1500	0	0	0	0	0	0	1990	1864	1800	1766	1743
119– 74	0	0	0	0	2200	1700	700	1200	0	0	0	0	2000	1841	1736	—	—
120– 29	0	0	0	7800	1500	2800	800	700	0	0	0	0	4540	4110	3880	3780	3686
– 26	4700	300	200	0	0	2000	0	0	0	0	0	0	2000	1905	1865	1828	1810
– 65	0	700	2100	4500	3200	2600	400	0	0	0	0	0	4240	3890	3750	—	—
–121	0	0	1400	6000	4300	800	400	1900	0	0	0	0	4800	4450	4210	4060	3980
121– 65	3500	3300	1880	0	1500	1500	0	0	0	0	0	400	3402	3245	3152	3100	3060
–104	0	3600	3350	0	4700	1500	700	500	0	0	0	0	4350	4100	3920	3828	—
43– 12	1000	1000	1780	500	0	300	0	0	0	0	1000	0	1550	1476	1445	1420	1400
– 23	2200	2400	480	0	1900	0	0	0	0	0	900	0	2190	2102	2039	—	—
– 41	1100	1500	630	250	0	250	0	0	0	0	1500	0	1435	1365	1032	—	—

Table 7. Calculated group velocities of Rayleigh waves for several periods in different dispersion regions.

T: Period in second.

N: Index of dispersion regions.

Values in parentheses: Group velocities (in km) of Rayleigh waves which belong to each standard dispersion curve.

n: Numbers of the observational equations.

a) Pacific area

N \ T	25	30	35
0	4.003±0.0095 (4.00)	4.075±0.0088 (4.08)	4.110±0.0180 (4.13)
1	3.939±0.0223 (3.91)	4.006±0.0209 (3.99)	4.029±0.0243 (4.03)
3	3.804±0.0277 (3.77)	3.928±0.0263 (3.86)	3.953±0.0312 (3.92)
5	3.550±0.0277 (3.50)	3.700±0.0269 (3.66)	3.794±0.0317 (3.76)
7	3.205±0.0371 (3.20)	3.340±0.0277 (3.36)	3.492±0.0312 (3.50)
A	3.923±0.0236 (3.98)	3.914±0.0270 (3.96)	3.920±0.0290 (3.91)
B	3.922±0.0162 (3.89)	3.785±0.0452 (3.87)	3.801±0.0465 (3.83)

b) Eurasia, Africa, Atlantic Ocean and Indian Ocean areas.

N \ T	20	25	30	35	40
0	3.812±0.0323 (3.85)	4.008±0.0195 (4.00)	4.087±0.0101 (4.08)	4.127±0.0127 (4.13)	4.172±0.0216 (4.16)
1	3.821±0.0350 (3.73)	3.915±0.0202 (3.91)	3.975±0.0101 (3.99)	4.011±0.0135 (4.03)	4.036±0.0210 (4.06)
3	3.514±0.0236 (3.55)	3.747±0.0155 (3.77)	3.882±0.0081 (3.86)	3.954±0.0108 (3.92)	4.003±0.0162 (3.94)
5	3.221±0.0189 (3.25)	3.489±0.0121 (3.50)	3.643±0.0065 (3.66)	3.727±0.0088 (3.76)	3.786±0.0123 (3.83)
6	3.140±0.0135 (3.10)	3.388±0.0081 (3.37)	3.536±0.0042 (3.52)	3.642±0.0058 (3.63)	3.736±0.0088 (3.71)
7	2.893±0.0088 (2.93)	3.183±0.0057 (3.20)	3.361±0.0030 (3.36)	3.492±0.0041 (3.50)	3.583±0.0061 (3.59)
8	2.784±0.0445 (2.78)	3.015±0.0256 (3.02)	3.226±0.0081 (3.24)	3.376±0.01.8 (3.40)	3.513±0.0155 (3.51)

(to be continued)

(continued)

N \ T	20	25	30	35	40
9	2.572±0.0364 (2.62)	2.787±0.0162 (2.87)	3.049±0.0088 (3.06)	3.252±0.0128 (3.26)	3.367±0.0182 (3.40)
10	2.793±0.0552 (2.49)	2.724±0.0262 (2.73)	2.954±0.0135 (2.98)	3.125±0.0196 (3.14)	3.238±0.0290 (3.30)
12	2.494±0.0579 (2.14)	2.503±0.0189 (2.46)	2.676±0.0088 (2.68)	2.871±0.0121 (2.85)	3.037±0.0189 (3.06)
B′	3.897±0.0702 (3.84)	3.959±0.0385 (3.88)	3.890±0.0182 (3.85)	3.897±0.0229 (3.81)	
C	3.711±0.0633 (3.82)	3.836±0.0358 (3.87)	3.848±0.0175 (3.89)	3.852±0.0229 (3.87)	
n	175	205	221	197	130

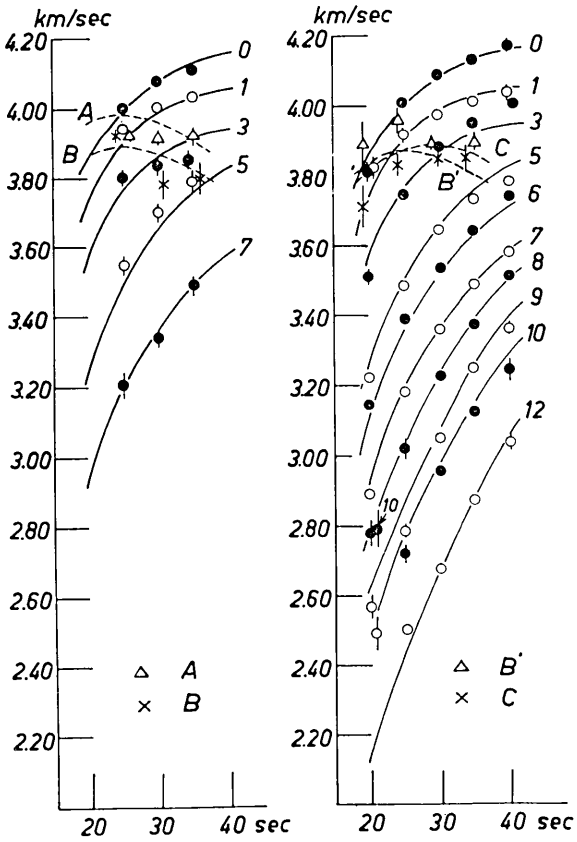

Fig. 3. Calculated group velocities of Rayleigh waves for each period in different dispersion regions. a) Pacific Ocean. b) An area including Eurasia, Africa, Atlantic Ocean and Indian Ocean. Vertical bar at each dot means the probable error.

any other. Suggested dispersion curves for these oceanic region must be revised in the future by adding much more data.

Except for these two special regions, the results of the calculation certificates the validity of our division pattern with regard to the regional dispersion characteristic of Rayleigh waves.

4. Discussions

The pattern in Fig. 5 has good concordance with the topography. A dispersion region "*12*" with the lowest group velocities, for instance, appear just at the Tibet Plateau, and the surrounding high mountainous districts and Alpen are also revealed to belong to dispersion region "*9*". In the oceans, on the other hand, regions "*0*" and "*1*" reasonably correspond to the deep ocean basins deeper than 5 km. Comparing with the results obtained from the propagation of *Lg* phase[26], the regions with the characteristic numbers less than "*3*" are considered to have a typically oceanic crustal structure missing a granitic layer[27]. North and South America, Greenland, Australia, Antarctica and its surrounding oceans are to be analysed at the next opportunity.

There are some exceptional regions, however, which must be discussed.

A) Rayleigh waves travelling through the continental shelf around Novaya Zemlya, inland seas of Baltic, Black and Carribean, show a mountainous type of dispersion with the characteristic numbers larger than "*9*". The dispersion region "*10*" had first to be placed in the Arctic Ocean between Novaya Zemlya to Scandinavia in order to explain the dispersion data of Rayleigh waves due to the atmospheric nuclear explosions[28),29] (see Fig. 4-a). These data compelled the writers to assume such an extraordinary region as "*10*" in the water-covered segments along the path. This strange supposition, however, was found to be quite satisfactory in view of the dispersion data along the paths crossing the region in question. Two sets of data by Porkka[30] from Kamchatka to Sodankylä and to Uppsala, for instance, lie between "*7–8*" (Fig. 4).

26) J. Oliver, M. Ewing and F. Press, "Crustal Structure of the Arctic Regions from the Lg Phase," *Bull. Geol. Soc. Amer.*, **66** (1955), 1063.

27) *loc. cit.*, 10).

28) J. N. Brune, J. E. Nafe and J. E. Oliver, "A Simplified Method for the Analysis and Synthesis of Dispersed Wave Trains," *J. Geophys. Res.*, **65** (1960), 287.

29) M. Båth, "Seismic Records of Explosions—Especially Nuclear Explosions. Part III," *FOA 4 Report A 4270-4721*, (1962), 116.

30) *loc. cit.*, 6).

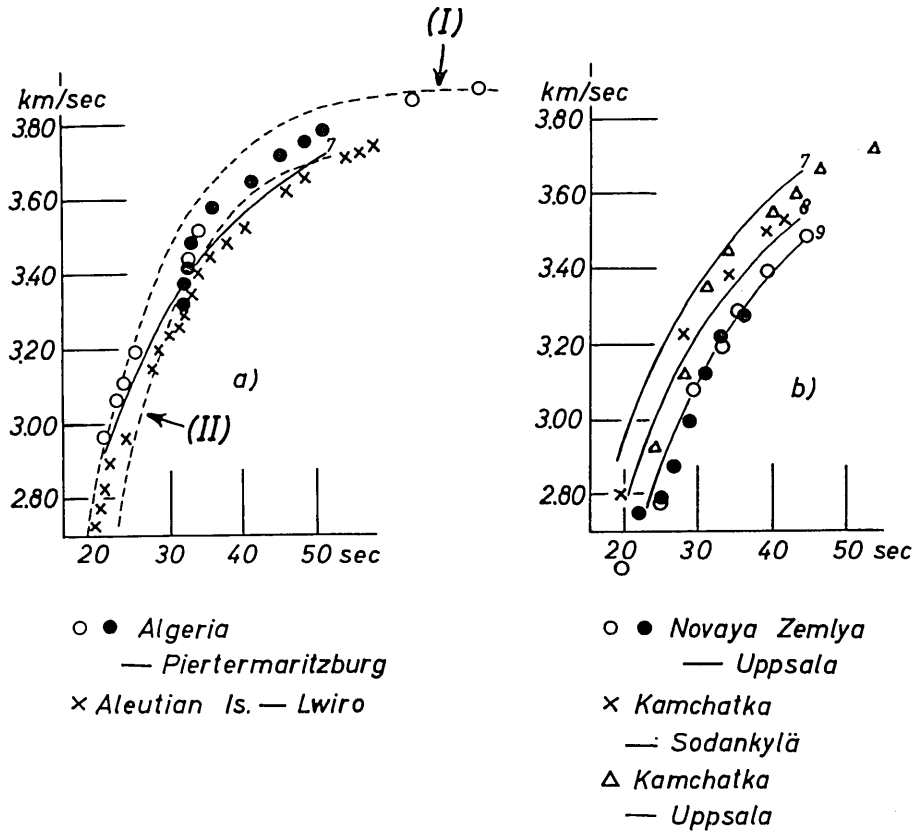

Fig. 4. Some examples of group velocity dispersion data of Rayleigh waves by other authors. a) Along African paths. b) Along continental margin paths between Novaya Zemlya and Scandinavia. Dashed curves: Theoretical dispersion curves (see p. 961). Solid curves: Standard dispersion curves.

The present writer's previous data at Uppsala[31] along the paths of ten shocks taking place in the active zone from Kamchatka to North of Honshu, Japan, also had such low velocities that they could also be well explained by the insertion of the region "*10*" in the region in question (Fig. 4). The necessity for placing the regions "*10*" and "*9*" in other inland seas was made clear in another paper[32].

31) *loc. cit.*, 7).
32) *loc. cit.*, 4).

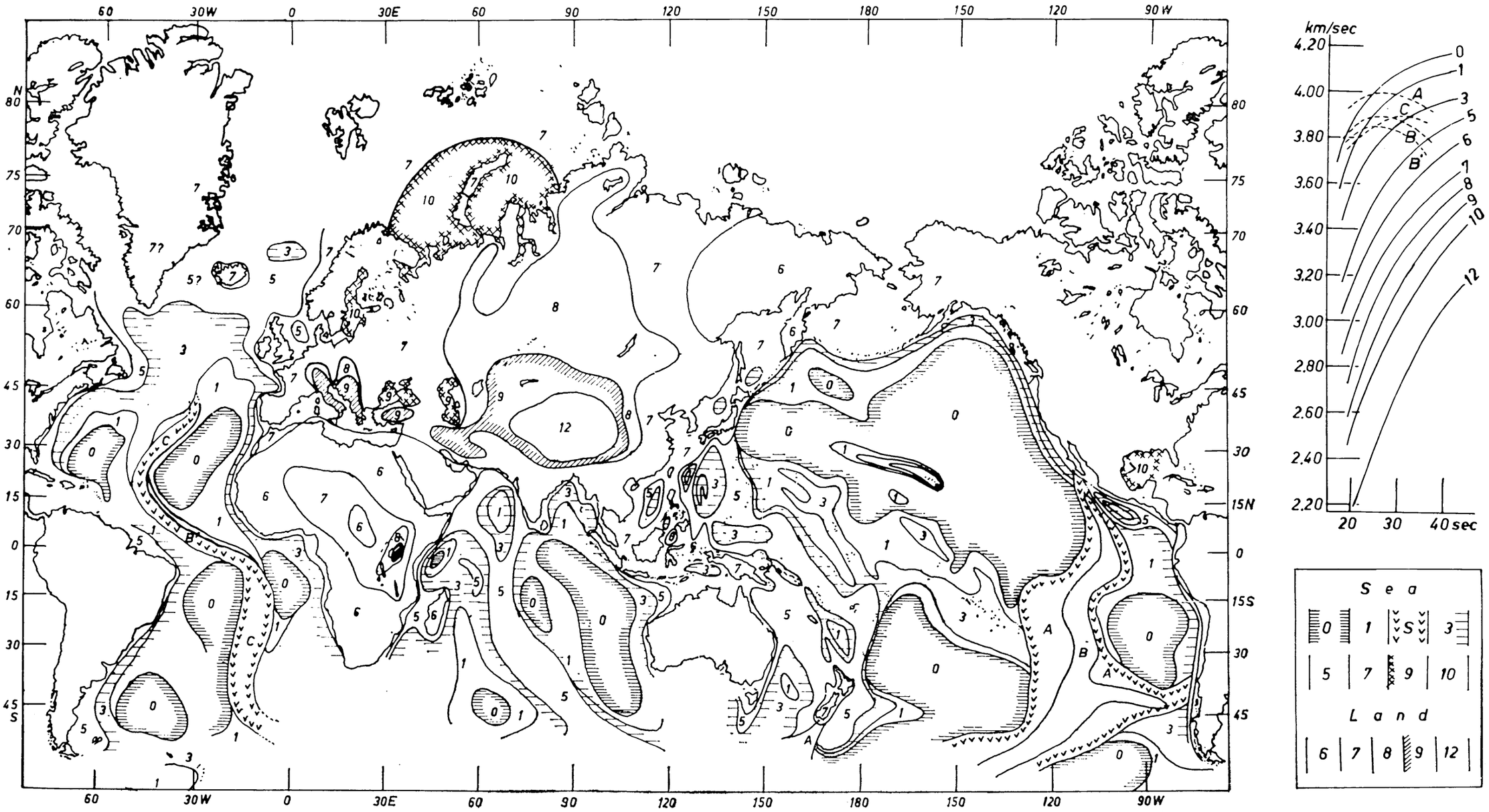

Fig. 5. Division map showing the regional characteristics of group velocity dispersion of Rayleigh waves. Standard dispersion curve representing the dispersion character in each region is given in the annexed diagram. In the legend, S means the special dispersion region with the dispersion characters of A, B, B' and C.

Of cause, we cannot suppose that the same crustal structure as in mountainous districts exists in such water-covered regions even if similar dispersion curves were obtained for them. One explanation for such unexpected results is found, too, in the crustal model of Dorman (case 8021, Table 8), which was used by Brune et al.[33], to explain the dispersion

Table 8. Crustal models used in this paper

h: Layer thickness in km. α: Compressional velocity in km/sec.
β: Shear wave velocity in km/sec. ρ: Density in gr/cm.^{3}

a) Model 6 EG

h	α	β	ρ
22	6.03	3.53	2.78
15	6.70	3.80	3.00
13	7.96	4.60	3.37
25	7.85	4.50	3.39
50	7.85	4.41	3.42
75	8.00	4.41	3.45
50	8.20	4.50	3.47
∞	8.40	4.60	3.50

b) Yamaguchi and Kizawa's model

h	α	β	ρ
1	1.50		1.0
20	5.00	2.89	2.8
∞	7.95	4.56	3.0

c) Dorman 8021

h	α	β	ρ
0.143H*	3.980	2.300	2.340
0.357H	6.150	3.500	2.817
0.500H	6.580	3.800	2.922
∞	8.140	4.700	3.300

(H*: Thickness of the crust)

data from Novaya Zemlya to Uppsala. After them, the crustal thickness (H) becomes about 40 km including an uppermost low velocity layer of about 5 km which also agrees well with their phase velocity data of dispersed Rayleigh waves. Looking at the model, the thickness of the crust of 35 km with usual seismic velocity is actually too thick considering the area is covered by water. A soft uppermost layer (α=3.98 km/sec, β=2.30 km/sec, ρ=2.34 gr/cc) with a rather large thickness of 5 km, however, seems to perform an effective role to make the dispersion of Rayleigh waves travelling the region in question similar to that of the mountainous area.

33) *loc. cit.*, 28).

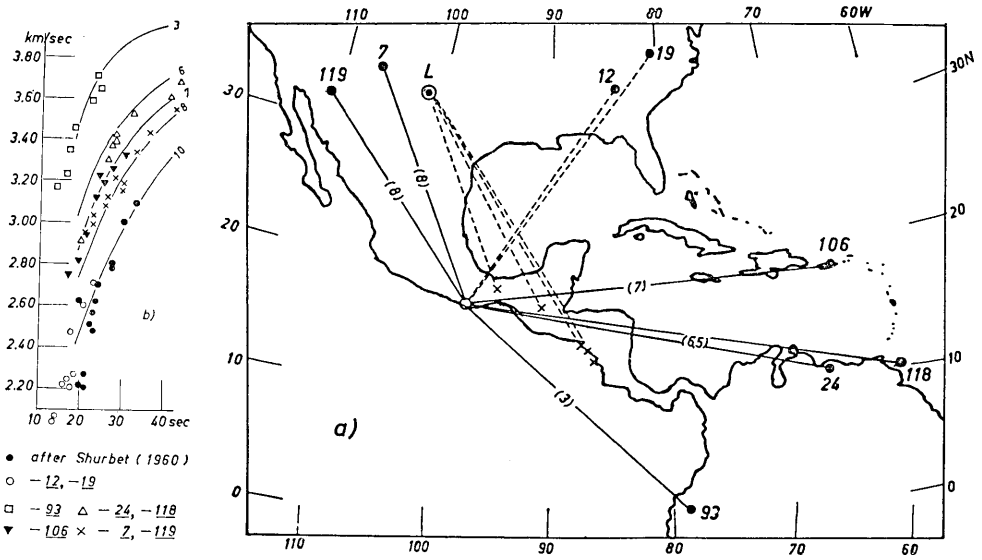

Fig. 6. Dispersion of Rayleigh wave group velocity along the paths in and around the Gulf of Mexico. a) Travelling paths. b) Dispersion data.

Since practically no sedimentary layer exists in Scandinavia, the thickness of this layer in the water-covered area increases, which is very roughly estimated as 5 km × (2200 km/1700 km) = 6.5 km, in which 2200 km and 1700 km are the lengths of total path and water-covered segment respectively along the path from the source to Uppsala. A soft sedimentary layer of similar thickness 7 km was also reported to exist in the Gulf of Mexico by Shurbet[34] from observations of Rayleigh wave dispersion. It is of interest to note that the dispersion of Rayleigh waves which he obtained along several paths crossing the Gulf area (Fig. 6-a), closely agrees with the curve "*10*" (Fig. 6-b). An additional investigation on the group velocity of Rayleigh waves due to a Mexican shock along the paths crossing the Gulf was also quite agreeable with Shurbet's result. Though the periods are restricted to a rather short range, the dispersion along the two paths crossing the Gulf (Fig. 6-b) differs significantly from the dispersion along any other path, but agrees well with the

34) D. H. SHURBET, "The Effect of the Gulf of Mexico on Rayleigh Wave Dispersion," *J. Geophys. Res.*, **65** (1960), 1251.

curve "*10*". Accumulation of the gravity data in the ocean[35] tells us that the sedimentation of soft superficial layer ($\rho=2.30-2.40$ gr/cc) with the thickness of more than several kilometers is not very rare.

B) There are such areas in the continents through which the Rayleigh wave dispersion has the characteristic number "*6*". This means the area is "*less continental*" than the shallow-covered areas which usually have the characteristic number "*7*"[36]. The dispersion data by Press et al.,[37] which have often been referred to as a standard continental dispersion (Fig. 4), also demand the segment of dispersion region "*6*" with length 3460 km beside another segment of "*7*" with length 4400 km along the path from Argeria to Pietermaritzburg.

Standard curve "*7*" was frequently observed by one of the present authors along many paths in the shallow sea regions with depth of less than 1000 m. The existence of the region "*6*", that is, the existence of a less continental dispersion region in the continent, however, is not surprising. As was demonstrated in this section, body wave velocity in the crust has a great influence upon the dispersion character, which fact can be seen in Fig. 4-a). The upper theoretical curve (I) corresponds to the crustal model 6EG (see Table 8) with crustal thickness of 37 km, which was adopted by Press[38] to fit his dispersion data of 1956. (A little thicker crustal thickness seems more preferable.) The lower theoretical curve (II) is by Yamaguchi et al.[39] with a crust of only 20 km overlaid by a water layer of 1 km thickness. The latter, in spite of the crustal thickness about half of the former, has a dispersion curve much more continental than the former and fits the standard curve "7". These two models are characterised by rather high velocity crustal layers of 6.03 km/sec and 6.70 km/sec and by a low velocity crustal layer of 5 km/sec respectively. The point is that the velocity in the crust is also quite effective to change the dispersion character of Rayleigh waves. This demonstration is instructive, in so far that we must not

35) J. L. Worzel, *Pendulum Gravity Measurements at Sea 1936-1959*. John Wiley & Sons, New York, (1965).

36) T. Santô, "Lateral Variation of Rayleigh Waves Dispersion Character. Part III. Atlantic Ocean, Africa and Indian Ocean," *Pure and Applied Geophysics*, **63** (1966), 40.

37) F. Press, "Crustal Structure in the California-Nevada Region," *J. Geophys. Res.*, **65** (1960), 1039.

38) *loc. cit.*, 37).

39) R. Yamaguchi and T. Kizawa, "Surface Waves and Layered Structure, Part 2. Theoretical Dispersion Curves for the Suboceanic Surface Waves," *Bull. Earthq. Res. Inst.*, **39** (1961), 669.

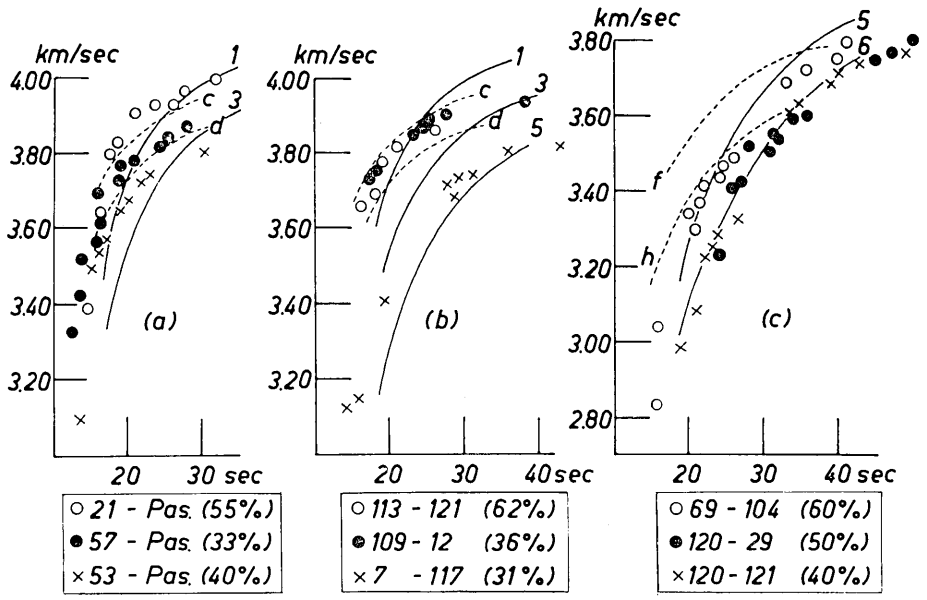

Fig. 7. Dispersion characters of Rayleigh waves along the paths crossing over a) East Pacific Rise, b) Mid-Atlantic Ridge and c) Mid-Indian Rise and Carlesberg Ridge. Length of segment covering each ridge is presented in brackets as percentage for total length.

carelessly assume crustal thickness from a comparison of the two dispersion curves, one along a continental path and the other along an oceanic path.

With regard to the existence of dispersion region "*6*" in the stable masses of Africa, Arabian Peninsula and East Siberia, another investigation made by J. Brune et al.[40] is quite interesting. They also found relatively high shear velocities in the crust as well as in the upper mantle from the phase and group velocities of Love waves in another stable mass, the Canadian shield.

Together with the discussion given in the previous section, we can say that dispersion of Rayleigh waves travelling along the continental shelf or inland sea becomes more or less "continental" due to the superficial

40) J. BRUNE and J. DORMAN, "Seismic Waves and Earth Structure in the Canadian Shield," *Bull. Seism. Soc. Amer.*, **53** (1963), 167.

soft layer. Further, we may say that stable mass changes the dispersion character of surface waves rather "oceanic" due to the relatively high seismic wave velocities in their crust-mantle system. We therefore make Table 9 showing the relation between the dispersion characterstic number and the crustal type.

Table 9. List of dispersion type.

Water-covered area		Land area	
Range of dispersion index	Type	Range of dispersion index	Type
<1.5	Deep oceanic		
1.6~3.5	Oceanic		
3.6~5.5	Oceanic transitional	6.0~6.5	Stable continental
5.6~7.5	Continental shelf	6.6~7.5	Low-land
>7.6	Thick sedimentary	7.6~9.4	Mountainous
		>9.5	High mountainous

C) Special dispersion charateristics of Rayleigh waves could hardly be recognized along the paths covering the Ridges in the Indian Ocean.

Rayleigh wave along the paths containing a considerable fraction of Ridge segments showed exceptional type of dispersion characteristics in both cases of East Pacific Rise[41] and Mid-Atlantic Ridge[42] (Fig. 7-a), -b)). The results seem to have a good correlation with a special crust-mantle system suggested by other geophysical surveys along these oceanic ridges. It has also been suggested that the Mid-Indian Rise and the Carlesberg Ridge are a continuation of the Mid-Atlantic Ridge with similar crustal structure. It was therefore expected that any special type of dispersion characteristic found on the Mid-Atlantic Ridge could be also observed along the paths through the Ridge and/or Rise in the Indian Ocean. Despite this expectation the result was negative (Fig. 7-c). These follow the standard curves "*5*" and "*6*" but not the special dispersion

41) *loc. cit.*, 20).
42) *loc. cit.*, 10),

curves "f" or "h". The special dispersion characteristics only appears slightly along the path from the shock 69 to the station 104. The present result demands more detailed checks with regard to the similarity of the crustal structure of Indian Rise with Mid-Atlantic Ridge and/or East Pacific Rise. Two recent results from different way of approach[43),44)] will be worth refering to here, which also did not require any special crust-mantle system under the Carlesberg Ridge.

49. レーリー波群速度の地理的分布

国際地震工学研修所 三東哲夫
地震研究所 佐藤泰夫

以前，太平洋海域についてレーリー波群速度の地理的分布をしらべたが，その時と同じ方法を用いて，今度はユーラシア，アフリカ両大陸，大西洋，印度洋両海域を含む広範な地域を，より多くの分散領域（夫々の領域内ではレーリー波が同一の分散性を示す領域）に分けることを試みた．夫夫の分散曲線は，第5図に示した通りである．更に，こうして分けられた各領域内でのレーリー波の群速度をかりに未知として，各周期毎（20秒，25秒，30秒，35秒，40秒）の群速度を最小自乗法によって算出してみた結果，さきに各々の領域中に仮定した群速度の値と極めてよく一致した値がえられ，はじめに仮定した分散性や，分割図（第5図）が共に正しいことが立証された．以前の太平洋海域についての結果に対しても，同じ様な計算を今回行ってみたが，之もまた同様な結果であった（第7表及び第3図）．

得られた分割図の様子は，全体としてほゞ地勢から想像される地殻の厚さの変化に順応している様に見える．然し同時に，次の様な予期に反した注目すべき結果も現われた．

a) アフリカ大陸の大半，アラビヤ半島の全部，シベリヤの北東部では，レーリー波は他の多くの大陸棚を伝わる場合よりも「海洋的」な分散性を示す．

このことは，之等の安定大陸のかたい地殻内での地震波速度が普通以上に速いこと，之に反して大陸棚中の地殻内では，表面の軟らかい堆積層の存在のために地震波の速度が普通よりもおそくなり，そのえいきょうが地殻の厚さのちがい以上にレーリー波の分散に大きくひゞいたためと考えられる．

b) ノバヤ・ゼムリヤ島周辺の北極海域，バルチック海の北部，黒海やカスピ海などの内海を通るレーリー波の分散は，山岳地帯を通る場合と同じ分散性を示す．

このことも又，これらの海域中での極端に厚い（数キロメートル又はそれ以上）軟弱な堆積層のえいきょうによるとすれば説明がつく．又，

c) 大西洋中央海嶺は，東太平洋海嶺と似た特殊な分散領域になっていることが分った．これに反し，印度洋海嶺には上の二つの海嶺中にみられた特殊なレーリー波の分散性をはっきり認めることは出来なかった．

43) J. G. F. Timothy and G. G. Shor, Jr, "Seismic Refraction Measurements in the Northwest Indian Ocean," *J. Geophys. Res.*, **71** (1966), 427.

44) F. S. Birch and A. J. Halunen, Jr, "Heat-Flow Measurements in the Atlantic Ocean, Indian Ocean, Mediterranean Sea, and Red Sea," *J. Geophys. Res.*, **71** (1966), 583.